Patterning nucleation area by femtosecond laser in exchange-coupled systems

Pierre Vallobra, Y Xu, H Wang, Grégory Malinowski, M Hehn, J-C Rojas-Sánchez, S Mangin

RESEARCH ARTICLE | SEPTEMBER 13 2023

Patterning nucleation area by femtosecond laser in exchange-coupled systems

P. Vallobra ; Y. Xu ; H. Wang ; G. Malinowski ; M. Hehn ; J.-C. Rojas-Sánchez ; S. Mangin

Appl. Phys. Lett. 123, 112406 (2023)
https://doi.org/10.1063/5.0157754

Applied Physics Letters ARTICLE pubs.aip.org/aip/apl

Patterning nucleation area by femtosecond laser in exchange-coupled systems

Cite as: Appl. Phys. Lett. **123**, 112406 (2023); doi: 10.1063/5.0157754
Submitted: 10 May 2023 · Accepted: 26 August 2023 ·
Published Online: 13 September 2023

P. Vallobra,[1,2] Y. Xu,[1,2,3] H. Wang,[2,3] G. Malinowski,[1] M. Hehn,[1] J.-C. Rojas-Sánchez,[1] and S. Mangin[1,a)]

AFFILIATIONS

[1]Institut Jean Lamour (UMR 7198), Université de Lorraine, Vandoeuvre-lès-Nancy, France
[2]Hefei Innovation Research Institute, Beihang University, Hefei 230013, China
[3]MIIT Key Laboratory of Spintronics, School of Integrated Circuit Science and Engineering, Beihang University, Beijing 100191, China

[a)]**Author to whom correspondence should be addressed:** stephane.mangin@univ-lorraine.fr

ABSTRACT

Optical control of the exchange bias field in IrMn/$[Co/Pt]_N$ heterostructures has been recently demonstrated. We show that this phenomenon can be used to create specific nucleation areas and even decide the preferential direction of propagation of the domain wall inside these preferred areas of nucleation. Using different features of a femtosecond laser, such as the helicity, fluence, and number of pulses, we designed robust patterns of various shapes and magnetic properties that can be host for domain wall propagation observations. Our finding provides an alternative method to already existing and time-consuming patterning methods.

In magnetic materials, the downsizing of MRAM is bound to reach a limit. To overcome this problem, Parkin *et al.* proposed in 2008 a new disruptive geometry, the domain wall racetrack memory.[1] This date marks the beginning of a global interest of the scientific community toward domain walls motion in magnetic racetracks.[2–4] The motion of other magnetic objects is not limited to domain wall since it can include among others skyrmions or superparamagnetic microbeads.[5–9] The standard way to control and confine the transport of magnetic objects is to pattern a thin film into stripes by conventional lithography and etching.[10,11] Those steps are time and energy consuming. In order to overcome those limitations, several groups demonstrated that it is possible to locally modify the magnetic properties either by thermally assisted scanning probe lithography,[12] electron irradiation,[13,14] or ion irradiation.[15,16] Many of those techniques are based on the modifications of the material properties, such as magnetic anisotropy or Dzyaloshiinsky–Moriya constant,[17] because those changes are robust and permanent, contrary to the magnetization direction in a ferromagnetic (FM) material.

Predicted by Neel in 1936 (Ref. 18) and exhibited for the first time in 1938 by Bizette,[19] antiferromagnetic (AFM) materials have since attracted increasing attention. Indeed, their null magnetic moment allows for an increased stability of their magnetic configuration. Thus, they became primary candidates for applications in magnetic memories and the manipulation of their magnetic configuration developed as a major area of study.[20–23] The recent demonstrations of AFM manipulation with spin transfer torque[24–26] and spin torque[27,28] are further proofs of this enthusiasm from the scientific community. AFM materials are currently used on an industrial scale in magnetic random access memories[29] and magnetoresistive heads[30] because they allow for the emergence of an exchange bias field (H_{EB}). This phenomenon that has been first uncovered by Meiklejohn and Bean in 1956 (Ref. 31) occurs in AFM/FM heterostructures where the hysteresis loop of the FM layer is shifted of a value H_{EB} due to the local exchange interactions with the interfacial AFM moments. While the standard way of setting the exchange bias fields consists in an annealing above the blocking temperature, we have recently demonstrated that it can also be achieved with ultra-short polarized laser pulses.[32] The possibility of manipulating magnetization using the helicity of femto-second laser pulses has been demonstrated in 2007[33] and continues to be studied.[34] Using this method, the exchange bias field could even be modified with one pulse of 50 fs, opening perspectives for ultrafast modification of magnetic properties. Note that in this paper, we demonstrate that femtosecond laser can be used in order to pattern areas of preferential domain nucleation in exchange-coupled bilayers by locally modifying the magnetic properties.

In this study, we prepared a Ta(3 nm)/Pt(5 nm)/IrMn(7 nm)/$[Co(0,6\,nm)/Pt(2\,nm)]_2$/Pt(3 nm) multilayer on a glass substrate

using dc magnetron sputtering with an Ar pressure lower than 5.5×10^{-8} mTorr.

We then performed optical excitation, using a Ti: sapphire fs-laser with a 5-kHz repetition rate, a wavelength of 800 nm (1.55 eV), and a pulse duration of 35 fs. The Gaussian beam was focused to 50 μm (FWHM) and swept with a velocity of 5 μm/s. A zero-order quarter-wave plate, which transformed linearly polarized light (L) into left-handed (σ^+) or right-handed (σ^-) circularly polarized light, controlled the helicity of the beam. The magnetic domains of the sample were studied using a static magneto-optic Faraday microscope while the laser was illuminating the sample. During the irradiation process, no external magnetic field is applied.

In order to investigate the nucleation and propagation of the magnetic domains, the sample was then moved to a magneto-optic Kerr effect (MOKE) microscope equipped with an electromagnet. Both the Faraday microscope used during the irradiation and the MOKE microscope used to investigate the domain properties are equipped with a 680-nm monochromatic high intensity LED that acts as a light source for imaging.

We measured the hysteresis cycle of the as-grown sample in the out-of-plane direction [Fig. 1(a)]. The sample displays a perpendicular magnetic anisotropy as well as an as-grown exchange bias field $H_{EB} < 0$.

Before carrying out the laser irradiation experiment, we saturated the sample magnetization with a positive out-of-plane magnetic field. We then swept the linearly polarized laser of 4.6 mJ/cm^2 on the sample. This laser fluence was below the critical fluence needed to reverse the magnetization of the Co/Pt with all optical switching (AOS). We could confirm that the magnetization of Co/Pt was not modified during the laser irradiation (not shown). After the laser irradiation, the hysteresis in the irradiated area was measured using MOKE microscope [Fig. 1(b)]. In the irradiated area, the exchange bias field increased after laser irradiation.

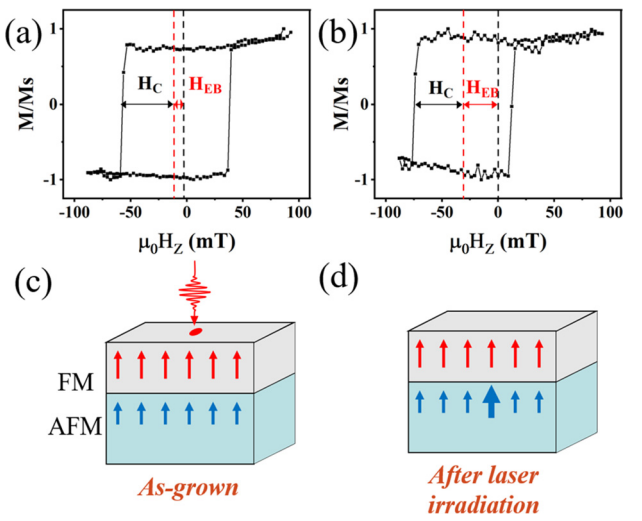

FIG. 1. Effect of the laser irradiation on the exchange bias. MOKE hysteresis loop of the exchanged biased sample (a) before and after and (b) laser irradiation. Configuration of the FM layer and the AFM interfacial uncompensated magnetic moments (c) before and (d) after laser irradiation.

The enhancement of the exchange field induced by laser pulses is explained in Figs. 1(c) and 1(d). According to the Meiklejohn model,[31] the exchange bias results from the interfacial uncompensated IrMn moments. In the as-grown state, our IrMn/[Co/Pt]$_2$ sample showed a weak exchange-bias field, indicating that interfacial moments of IrMn were almost compensated [Fig. 1(c)]. During the laser irradiation, the IrMn moments were heated by the femtosecond laser and then cooled in the presence of saturated FM moments. This allows for interfacial magnetic moments of IrMn to be pinned due to the Co–Mn exchange coupling. This mechanism is similar to the one obtained for synthetic ferrimagnet.[35] More interfacial magnetic moments at the IrMn/[Co/Pt]$_2$ interface led to a stronger exchange bias field after laser irradiation [Fig. 1(d)]. The highest EB value we achieved in this sample through laser irradiation is 31 mT, as depicted in Fig. 1(b). Various factors influence the EB value, including laser fluence and the thickness of IrMn. We opted for a 7 nm thickness of IrMn, aligning with the EB peak.[36] When employing lower laser fluences, like the 4.6 mJ/cm^2 used in this experiment, the Co/Pt remains largely unaffected by the laser. Meanwhile, the magnetization of IrMn at the interface reorients in alignment with the initial configuration of Co/Pt. Conversely, with higher fluences, helicity-dependent AOS emerges, causing both Co/Pt magnetization and IrMn moments at the interface to realign based on the helicity of the light. We then imaged the sample on the area previously exposed to the laser with a MOKE setup under some specific conditions. We saturated the sample with an out of plane negative field and imaged the domains while slowly increasing the field from −100 mT to the positive saturation field. These MOKE images can be seen in Figs. 2(a)–2(d).

In image Fig. 2(a), the applied magnetic field is 6.08 mT and the sample is still fully saturated down. When the field is increased, we can clearly observe in Figs. 2(b) and 2(c) that the location where the laser has been swept is now an area of preferential nucleation. As observed on Fig. 2(d), upon further increasing the magnetic field, the switching finally occurs in the rest of the sample.

To ensure that the irradiated area has strictly different properties than the rest of the sample, we saturated the sample with a positive out of plane field and then decreased the field while imaging as displayed in Figs. 2(e)–2(h). The uniformly saturated state is observed initially on image Fig. 2(e), and the switching occurs first in the non-irradiated area as it can be seen on images Figs. 2(f) and 2(g) at stronger magnitudes of the negative field. Upon further increasing the field magnitude, the switching finally starts to initiate in the irradiated area as observed in Fig. 2(h) until the whole sample magnetization is reversed (not shown).

With the above described method, we designed several other patterns of irradiated area as observed on Figs. 3(b)–3(d). Contrary to Figs. 3(a) and 3(b), the patterns designed on Figs. 3(c) and 3(d) needed the laser beam to go several times over the same area at the junction of multiple paths because of the complexity of the patterns. However, this does not affect the nucleation pattern. All those MOKE images show that with a femtosecond laser, it is possible to design any preferential nucleation shape, even by sweeping the laser several times on the same area.

In the next experiment, we aimed at creating an area with a gradient of exchange bias field. For this, we saturated the [Co/Pt] bilayer with a negative out of plane magnetic field and tuned different laser parameters to nonetheless create an area of nucleation but also set a

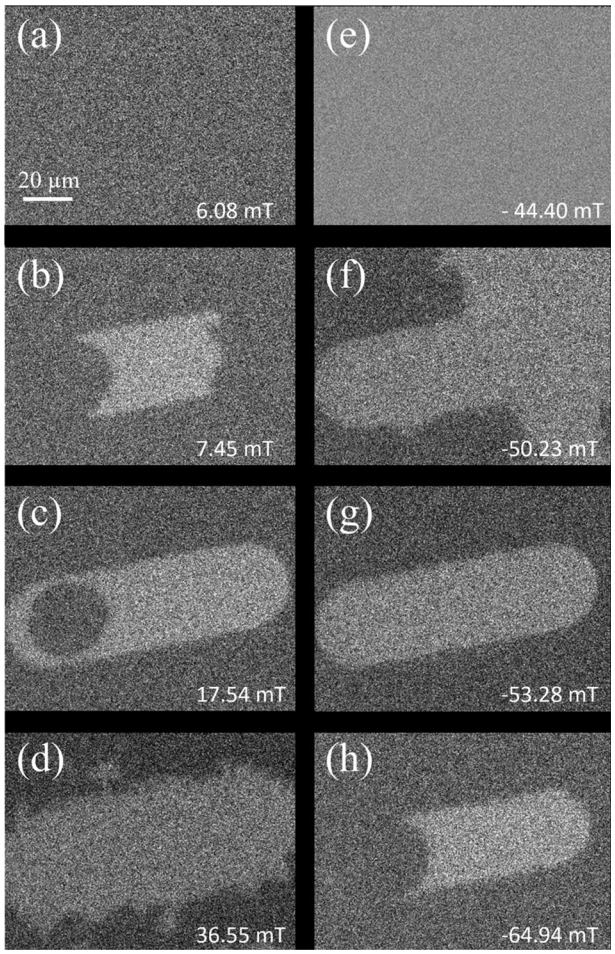

FIG. 2. Magnetic pattern of previously irradiated area. The sample has been first exposed to a linearly polarized laser with a fluence of 4.6 mJ/cm^2 and then moved to the MOKE microscope. It has then been saturated with a strong negative (respectively, positive) field. Then, the field has been increased (respectively, decreased) gradually to observe reversing magnetic domains from (a) to (d) [respectively, (e) and (f)].

specific direction of domain propagation. This experiment revolves around specific characteristics of the helicity-dependent AOS in Co/Pt. The helicity-dependent AOS in Co/Pt can only occur after a certain laser fluence threshold is reached because it initially requires inducing demagnetization. Following this demagnetization, the Co/Pt material remagnetizes either positively or negatively, depending on whether the helicity of the light is $\sigma+$ or $\sigma-$. Furthermore, the remagnetization process in Co/Pt necessitates multiple pulses to take effect. If the laser beam remains stationary during the AOS process, a distinct pattern emerges. At the center of the laser spot, where power is higher, a fully demagnetized circle forms. At the circle's edge, where power decreases, the remagnetization process is unimpeded, resulting in the switching phenomenon. This region is known as the "switching ring." In a previous study,[32] we demonstrated that using AOS for laser-induced EB writing is notably more effective in areas with higher Co/Pt magnetization. Specifically, this applies to the switching ring and when a larger

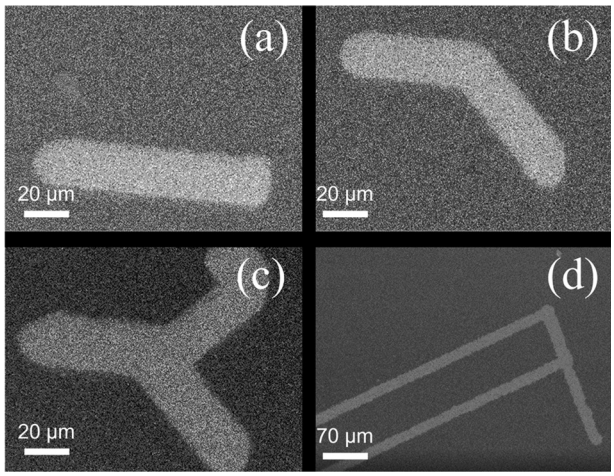

FIG. 3. Different shapes of magnetic pattern of previously irradiated area. The sample has been first exposed to a linearly polarized laser with a fluence of 4.6 mJ/cm^2 and then moved to a MOKE microscope. (a)–(d) are different pattern obtained by sweeping differently the laser on the sample.

number of laser pulses are utilized. Essentially, the EB value is greater when Co/Pt magnetization is more pronounced during laser exposure.

In this last experiment, we use the laser fluence, the helicity of the light, and the number of pulses as degrees of freedom. The laser fluence is of 9.6 mJ/cm^2, just above the switching threshold of the [Co/Pt] multilayer switching, and the helicity is $\sigma-$ to trigger the AOS effect in the direction of negative saturation. In the process, this number of pulses changes depending on the area as shown in Fig. 4(a). The procedure consists in sending a light pulse and moving the sample laterally, sending five light pulses and moving the sample laterally, sending 50 light pulses and moving laterally, and so on until 5000 pulses. Because the lateral displacement of the sample (20 μm) is smaller than the radii of the laser spot (25 μm), a part of the area that has been exposed to the first laser pulse is also exposed to the following five pulses as seen on Fig. 4. At the end of the procedure, the resulting area exposed to the laser has a shape similar to a line.

The point of this procedure lies in the fact that the exchange bias field increases with the number of laser pulses,[32] so a gradient of positive coercive field is expected to exist along the line from the area exposed to the first laser pulse to the area exposed to the last 5000 pulses. We measured the value of the positive magnetic field needed to saturate the magnetization positively for each position of the laser. The value of the positive coercive field as function of the number of pulses is displayed on Fig. 4(b). As expected, we observe a nonlinear increase in the coercive field with the number of pulses, yielding a spatial gradient of positive coercive field. The nonlinearity can be attributed to the consecutive two-step process of AOS in the Co/Pt layer. The initial step involves demagnetization, exhibiting linearity with the number of pulses. Subsequently, the second step follows, characterized by nonlinear, helicity-dependent remagnetization.[37]

Using MOKE microscope, we then imaged the region exposed to the laser as seen in Figs. 4(c)–4(h).

On the MOKE microscope, we first saturated negatively the sample and increased the value of the field from the negative to the positive

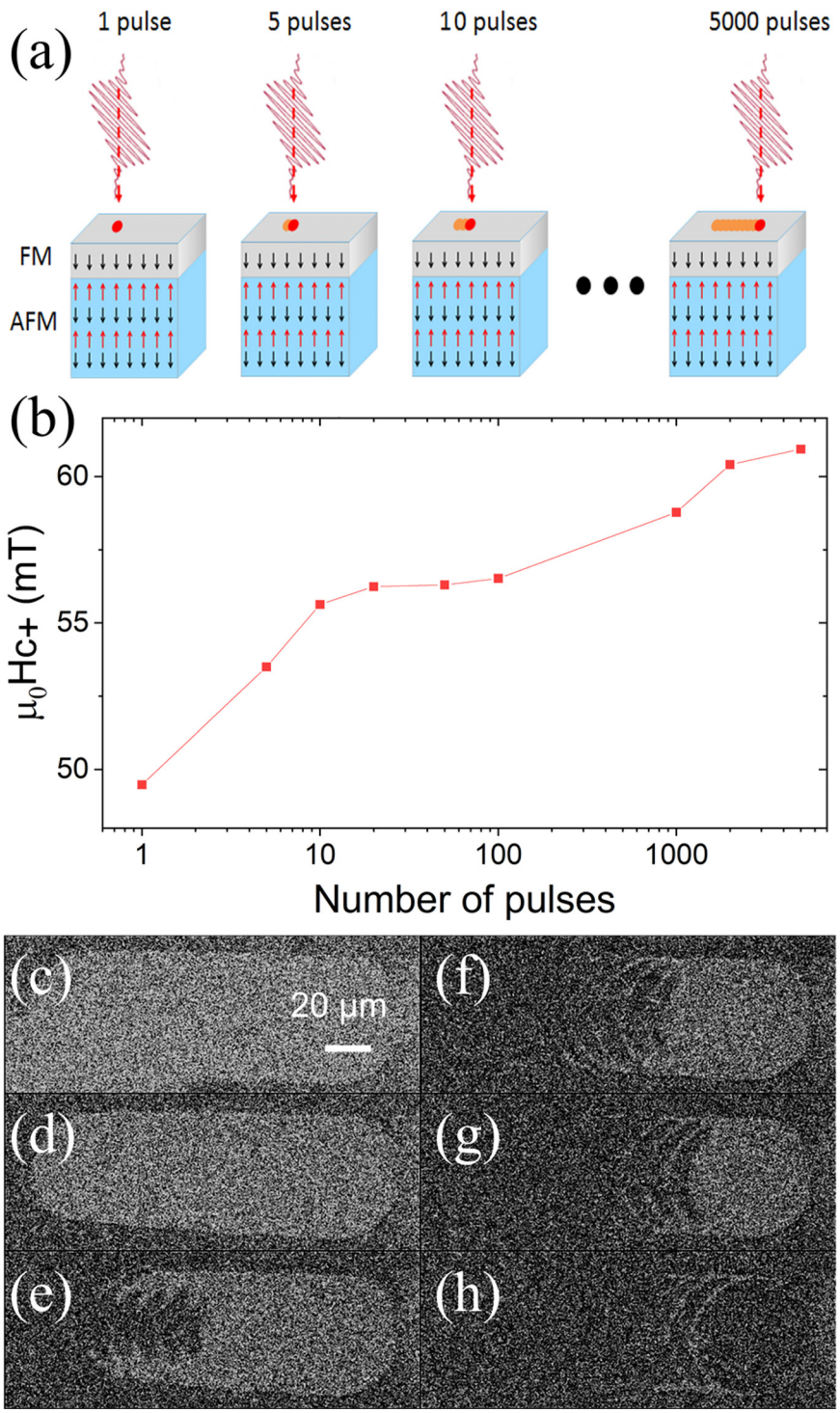

FIG. 4. Previously irradiated area exhibiting an exchange bias gradient. (a) Schematic of the experimental procedure. Starting from a negatively saturated ferromagnetic layer, a single laser pulse is sent on a virgin area on the sample. Then, the sample is moved laterally of 20 μm to send five laser pulses, move the laser laterally of 20 μm to send 10 pulses. This operation of lateral displacement of the sample and exposure to laser pulses has been repeated for 50, 100, 200, 500, 1000, 2000, and 5000 pulses. The laser fluence is 9.6 mJ/cm^2. Its polarization is σ^-. (b) Switching field at positive field (Hc+) as a function of the number of pulses. MOKE images of the sample at (c) 40.68, (d) 49.26, (e) 56.60, (f) 57.78, (g) 60.01, and (h) 61.15 mT.

to nucleate domains of positive magnetization as seen in Fig. 4(c) taken at 40.68 mT. The darker domains (respectively, clearer) are saturated positively (respectively, negatively). Coherently, the magnetization switching is first observed outside of the irradiated area since the laser exposition process tends to set the exchange bias field to a positive value. Indeed, in Fig. 4(d), at a 49.26 mT, we observe that domains of negative magnetization have reversed around the area previously exposed to the laser but not inside it.

As observed in Fig. 4(e) for 56.6 mT, the magnetization switching in the previously irradiated area occurs first on the left of the image, where the number of laser pulses was the lowest. This is due to the smaller modification of the exchange bias for fewer laser pulses. Interestingly, in Figs. 4(f) and 4(g), the outer rings appear as areas where the switching occurs at last. These outer rings are precisely where AOS of Co/Pt happens, resulting in a higher EB value compared to the center of the spot, where only demagnetization occurs. Furthermore, these outer rings are more stable with field, i.e., have a higher EB value, on the right of the images, where the number of pulse is the highest. This is unambiguously due to the fact that the remagnetization of the Co/Pt needs many pulses to occur. Thus, Fig. 4 clearly shows that we can use the switching ring at our advantage to tailor a specific pattern with a controlled domain propagation path.

Our method of patterning can be assimilated to maskless optical lithography. Thus, smaller pattern sizes available with maskless lithography are also accessible by our method. Furthermore, the possibility to create a gradient of exchange bias in irradiated areas is a supplementary degree of freedom that opens up a path for the observations of new modes of domain wall and skyrmion propagation. For instance, since the size of a skyrmion in a biased layer depends on the value of the exchange bias field,[38] our procedure could also allow for a fine tuning of the skyrmion size without any applied field and the creation of areas of different skyrmion sizes.

In conclusion, we have shown that it is possible to pattern specific areas of nucleation using femtosecond polarized light in a FM/AFM multilayer and even to impose a direction of propagation to the domain walls using pulses. The number of laser pulses, the helicity of the light, and its fluence are many factors that can be used to control precisely the domain wall propagation. This laser patterning method could have numerous applications since it is a very flexible way to create domain nucleation areas at any location of a sample. It paves the way for fast, precise, and controllable patterning and confined domain wall propagation.

The authors are grateful for the financial support from the National Natural Science Foundation of China (No 12250410245).

AUTHOR DECLARATIONS

Conflict of Interest

The authors have no conflicts to disclose.

Author Contributions

Pierre Vallobra: Data curation (equal); Formal analysis (equal); Investigation (equal); Methodology (equal); Validation (equal); Visualization (equal); Writing – original draft (equal); Writing – review & editing (equal). **Yong Xu:** Data curation (equal); Investigation (equal); Validation (equal); Visualization (equal); Writing – original draft (equal); Writing – review & editing (equal). **Huiwen Wang:** Writing – original draft (equal); Writing – review & editing (equal). **Gregory Malinowski:** Data curation (equal); Resources (equal); Writing – original draft (equal); Writing – review & editing (equal). **Michel Hehn:** Conceptualization (equal); Resources (equal); Supervision (equal); Writing – original draft (equal); Writing – review & editing (equal). **Juan-Carlos Rojas-Sánchez:** Data curation (equal); Resources (equal); Supervision (equal); Writing – original draft (equal); Writing – review & editing (equal). **Stéphane Mangin:** Conceptualization (equal); Methodology (equal); Resources (equal); Supervision (equal); Validation (equal); Writing – original draft (equal); Writing – review & editing (equal).

DATA AVAILABILITY

The data that support the findings of this study are available from the corresponding author upon reasonable request.

REFERENCES

[1]S. Parkin, M. Hayashi, and L. Thomas, Science **320**, 190 (2008).
[2]D. A. Allwood, G. Xiong, C. C. Faulkner, D. Atksinson, and R. P. Cowburn, Science **309**, 1688 (2005).
[3]A. Mougin, M. Cormier, J. P. Adam, P. J. Metaxas, and J. Ferré, Europhys. Lett. **78**, 57007 (2007).
[4]B. Cui, D. Li, J. Yun, Y. Zuo, X. Guo, K. Wu, X. Zhang, Y. Wang, L. Xi, and D. Xue, Phys. Chem. Chem. Phys. **20**, 9904 (2018).
[5]T. Schulz, R. Ritz, A. Bauer, M. Halder, M. Wagner, C. Franz, C. Pfleiderer, K. Everschor, M. Garst, and A. Rosch, Nat. Phys. **8**, 301–304 (2012).
[6]A. Fert, V. Cros, and J. Sampaio, Nat. Nanotechnol. **8**, 152–156 (2013).
[7]E. Rapoport and G. S. D. Beach, Sci. Rep. **7**, 10139 (2017).
[8]M. Ouk and G. S. D. Beach, J. Magn. Magn. Mater. **444**, 218–226 (2017).
[9]B. Dieny, I. L. Prejbeanu, K. Garello *et al.*, Nat. Electron. **3**(8), 446–459 (2020).
[10]M. A. Basith, S. McVitie, D. McGrouther, J. N. Chapman, and J. M. R. Weaver, J. Appl. Phys. **110**, 083904 (2011).
[11]I. Polenciuc, A. J. Vick, D. A. Allwood, T. J. Hayward, G. Vallejo-Fernandez, K. O'Grady, and A. Hirohata, Appl. Phys. Lett. **105**, 162406 (2014).
[12]E. Albisetti, D. Petti, M. Pancaldi, M. Madami, S. Tacchi, J. Curtis, W. P. King, A. Papp, G. Csaba, W. Porod, P. Vavassori, E. Riedo, and R. Bertacco, Nat. Nanotechnol. **11**, 545–551 (2016).
[13]A. V. Krasheninnikov and K. Nordlund, J. Appl. Phys. **107**, 071301 (2010).
[14]S. W. Han, Y. Park, Y. H. Hwang, W. G. Lee, and S. C. Hong, Appl. Phys. Lett. **109**, 252403 (2016).
[15]L. H. Diez, M. Voto, A. Casiraghi, M. Belmeguenai, Y. Roussigné, G. Durin, A. Lamperti, R. Mantovan, V. Sluka, V. Jeudy, Y. T. Liu, A. Stashkevich, S. M. Cherif, J. Langer, B. Ocker, L. Lopez-Diaz, and D. Ravelosona, Phys. Rev. B **99**, 054431 (2019).
[16]T. Devolder, J. Ferré, C. Chappert, H. Bernas, J.-P. Jamet, and V. Mathet, Phys. Rev. B **64**, 064415 (2001).
[17]A. Sud, S. Tacchi, D. Sagkovits, C. Barton, M. Sall, L. H. Diez, E. Stylianidis, N. Smith, L. Wright, S. Zhang, X. Zhang, D. Ravelosona, G. Carlotti, H. Kurebayashi, O. Kazakova, and M. Cubukcu, Sci. Rep. **11**, 23626 (2021).
[18]L. Néel, Ann. Phys. **10**, 5 (1932).
[19]H. Bizette, C. F. Squire, and B. Tsai, C. R. Acad. Sci. **207**, 449 (1938).
[20]A. S. Nunez, R. A. Duine, P. Haney, and A. H. MacDonald, Phys. Rev. B **73**, 214426 (2006).
[21]P. M. Haney and A. H. MacDonald, Phys. Rev. Lett. **100**, 196801 (2008).
[22]H. V. Gomonay and V. M. Loktev, Phys. Rev. B **81**, 144427 (2010).
[23]M. Bode, E. Y. Vedmedenko, K. von Bergmann, A. Kubetzka, P. Ferriani, S. Heinze, and R. Wiesendanger, Nat. Mater. **5**, 477 (2006).
[24]T. Jungwirth, X. Marti, P. Wadley, and J. Wunderlich, Nat. Nanotechnol. **11**, 231 (2016).
[25]R. Cheng and Q. Niu, Phys. Rev. B **89**, 081105(R) (2014).
[26]E. G. Tveten, A. Qaiumzadeh, and A. Brataas, Phys. Rev. Lett. **112**, 147204 (2014).
[27]P. Wadley, B. Howells, J. Zelezny, C. Andrews, V. Hills, R. P. Campion, V. Novak, F. Freimuth, Y. Mokrousov, A. W. Rushforth, K. W. Edmonds, B. L. Gallagher, and T. Jungwirth, Science **351**, 587 (2016).
[28]S. Peng, D. Zhu, W. Li, H. Wu, A. J. Grutter, D. A. Gilbert, J. Lu, D. Xiong, W. Cai, P. Shafer, K. L. Wang, and W. Zhao, Nat. Electron. **3**, 757–764 (2020).
[29]D. Apalkov, B. Dieny, and J. M. Slaughter, Proc. IEEE **104**, 1796 (2016).
[30]E. E. Fullerton and J. R. Childress, Proc. IEEE **104**, 1787 (2016).
[31]W. H. Meiklejohn and C. P. Bean, Phys. Rev. **102**, 1413 (1956).
[32]P. Vallobra, T. Fache, Y. Xu, L. Zhang, G. Malinowski, M. Hehn, J.-C. Rojas-Sánchez, E. E. Fullerton, and S. Mangin, Phys. Rev. B **96**, 144403 (2017).

[33]C. D. Stanciu, F. Hansteen, A. V. Kimel, A. Kirilyuk, A. Tsukamoto, A. Itoh, and T. Rasing, Phys. Rev. Lett. **99**, 047601 (2007).
[34]Y. Xu and S. Mangin, J. Magn. Magn. Mater. **564**, 170169 (2022).
[35]J. W. Liao, P. Vallobra, L. O'Brien, U. Atxitia, V. Raposo, D. Petit, T. Vemulkar, G. Malinowski, M. Hehn, E. Martínez, S. Mangin, and R. P. Cowburn, Adv. Sci. **6**(24), 1901876 (2019).
[36]G. Vallejo-Fernandez, L. Fernandez-Outon, and K. O'Grady, J. Phys. D **41**, 112001 (2008).
[37]M. El Hadri, M. Hehn, P. Pirro, C.-H. Lambert, G. Malinowski, E. Fullerton, and S. Mangin, Phys. Rev. B **94**, 064419 (2016).
[38]W. Legrand, D. Maccariello, F. Ajejas, S. Collin, A. Vecchiola, K. Bouzehouane, N. Reyren, V. Cros, and A. Fert, Nat. Mater. **19**, 34–42 (2020).